Published in final edited form as:
Bone. 2012 April ; 50(4): 901–908. doi:10.1016/j.bone.2011.12.019.

MURINE AMELOBLASTS ARE IMMUNONEGATIVE FOR TCIRG1, THE V-H-ATPase SUBUNIT ESSENTIAL FOR THE OSTEOCLAST PLASMA MEMBRANE PROTON PUMP

Antonius LJJ Bronckers[1], **Donacian M Lyaruu**[1], **Theodore J Bervoets**[1], **Juan F Medina**[2], **Pamela DenBesten**[3], **Johan Richter**[4], and **Vincent Everts**[1]

[1]Dept of Oral Cell Biology ACTA, University of Amsterdam and VU University Amsterdam, Research Institute MOVE, Gustav Mahlerlaan 3004 Amsterdam The Netherlands [2]Division of Gene Therapy and Hepatology, University Hospital/School of Medicine/CIMA, University of Navarra, and Ciberehd, Pamplona, Spain [3]Dept of Orofacial Sciences, School of Dentistry, University of California at San Francisco, CA, USA [4]Molecular Medicine and Gene Therapy, Lund Stem Cell Centre, University of Lund, Lund, Sweden

Abstract

Maturation stage ameloblasts of rodents express vacuolar type-H-Atpase in the ruffled border of their plasma membrane in contact with forming dental enamel, similar to osteoclasts that resorb bone. It has been proposed that in ameloblasts this v-H-Atpase acts as proton pump to acidify the enamel space, required to complete enamel mineralisation. To examine whether this v-H-Atpase in mouse ameloblasts is a plasma membrane proton pump, we determined whether these cells express the lysosomal, T-cell, immune regulator 1 (Tcirg1, v-H-Atp6v$_0$a$_3$), which is an essential part of the plasma membrane proton pump that is present in osteoclasts. Mutation of this subunit in *Tcirg1* null (or *oc/oc)* mice leads to severe osteopetrosis. No immunohistochemically detectable Tcirg1 was seen in mouse maturation stage ameloblasts Strong positive staining in secretory and maturation stage ameloblasts however was found for another subunit of v-H-Atpase, subunit b, brain isoform (v-H-Atp6v$_1$b$_2$). Mouse osteoclasts and renal tubular epithelium stained strongly for both Tcirg1 and v-H-Atp6v$_1$b$_2$. In *Tcirg1* null mice osteoclasts and renal epithelium were negative for Tcirg1 but remained positive for v-H-Atp6v$_1$b$_2$. The bone in these mutant mice was osteopetrotic, tooth eruption was inhibited or delayed, and teeth were often morphologically disfigured. However, enamel formation in these mutant mice was normal, ameloblasts structurally unaffected and the mineral content of enamel similar to that of wild type mice.

We concluded that Tcirg1, which is essential for osteoclasts to pump protons into the bone, is not appreciably expressed in maturation stage mouse ameloblasts. Our data suggest that the reported v-H-Atpase in maturation stage ameloblasts is not the typical osteoclast-type plasma membrane associated proton pump which acidifies the extracellular space, but rather a v-H-Atpase that potentially is involved in intracellular acidification.

Correspondence to: Antonius LJJ Bronckers, Dept of Oral Cell Biology, ACTA, Gustav Mahlerlaan 3004, 1081 LA Amsterdam, Tel: +31-20-5980229; a.bronckers@acta.nl.

Keywords

ameloblasts; v-H-Atp6v$_0$a$_3$; v-H-Atp6v$_1$b$_2$; Tcirg1; pH regulation

Introduction

Ameloblasts are epithelial cells that produce dental enamel principally in two stages. In the first (secretory) stage they deposit a protein-rich enamel matrix that provisionally mineralizes. In the second (maturation) stage the cells transform into cells with resorbing characteristics and periodically form a ruffled border in the apical plasma membranes facing the enamel space. The matrix in the enamel space is proteolytically degraded by enzymes such as MMP20 and kallikrein 4 (KLK4) secreted by the ameloblasts. The hydrolyzed matrix fragments are gradually removed from the enamel space, where simultaneously apatite crystals rapidly expand until enamel mineralization is completed and the tooth erupts [1, 2].

Maturation ameloblasts have some structural similarity with osteoclasts, the bone resorbing cells. Both cell types have an actin-rich ruffled border [3, 4] that can endocytose, resorb and digest extracellular matrix components, *i.e.* the forming enamel below ameloblasts [1, 2], and the bone below osteoclasts [4, 5]. However, with respect to the inorganic apatite mineral, the cells perform opposite functions. Ameloblasts are involved in *formation* of minerals in enamel at a pH that periodically alternates between 6.0 and 7.2 [6, 7], whereas the osteoclasts *dissolve* the minerals of bone by acidifying the bone to which they are attached [4, 5]. To dissolve bone mineral the osteoclast generates protons by the activity of intracellular carbonic anhydrase [4, 5, 8]. These protons are subsequently pumped into resorption pits that form beneath the osteoclast, a process mediated by a vacuolar type of H-ATPase located in the plasma membrane [9, 10]. To control intracellular pH the osteoclast uses a set of pH regulators in its membrane [8,11–13].

Recent data show that maturation ameloblasts also have a pH regulatory machinery, quite similar to osteoclasts [14–17]. Immunohistochemical staining shows that also the ruffled border of rat incisor maturation stage ameloblasts is rich in v-H-Atpase [14, 16]. In osteoclasts this v-H-Atpase is a proton pump to acidify the resorption pits, but its function in maturation ameloblasts has not been resolved. Several groups speculated that in analogy to osteoclasts the v-H-Atpase in maturation stage ameloblasts acts as a proton pump to acidify the enamel space [14–16]. This would prevent mineralization of the enamel surface and enables diffusion of mineral ions into deeper layers as long as these are not yet fully mature [16]. An alternate view of pH regulation proposes that maturation ameloblasts secrete bicarbonates into the forming enamel to buffer protons released by crystal growth [1, 2, 17–19]. In this model the v-H-ATPase in the ruffled border of ameloblasts would be associated with intracellular acidification, rather than serving as a plasma membrane proton pump.

In the present study we addressed two questions: First, does the ruffled border of mouse maturation stage ameloblasts contain typical osteoclast like-proton pump subunits? Secondly, are ameloblasts affected and is enamel mineralisation incomplete when the typical osteoclast plasma proton pump is non-functional? To answer these questions we first tested if ameloblasts are immunopositive for the T-cell immune regulator 1 (Tcirg1; also called Atp6v$_0$a$_3$ subunit). This subunit is a 116 kDa protein that is abundantly present in the ruffled border of acid- secreting osteoclasts and intercalating cells of acid-secreting renal tubular epithelium, where it forms an essential part of the transmembrane proton translation domain v$_0$ of the v-H-Atpase [20, 21]. Its absence results in the dysfunction of osteoclasts leading to a severe osteopetrotic phenotype found in the *Tcirg1* null (*oc/oc)* mouse [4, 9, and 20]. We

furthermore localized the $Atp6v_1b_2$ subunit, also associated with murine osteoclasts [22]. Finally, we examined the effect of the disruption of the *Tcirg1* gene on enamel formation and on enamel mineral content in the *Tcirg1* null mouse. As positive control for enamel defects caused by disruption of pH regulation we used the anionic exchange -2 ($Ae2_{a,b}$) null mutant mouse model [15].

Materials and Methods

Animals and tissues

The *Tcirg1* null mice (background: C57BL/6J_C3HheB/FeJ) were obtained from Jackson Laboratories (Bar Harbor, ME, USA). Mutation in the *Tcirg1* null mouse is caused by a spontaneous 1.6 kp deletion starting in the middle of intron 1 and extending 62 bp into exon 3 in the genomic DNA. The deletion removes the translation start site of *Tcirg1* at the beginning of exon 2 [20]. Affected animals exhibit the characteristic radiologic and histologic features of osteopetrosis, including a generalized increase in skeletal density, absence of major marrow cavities and failure of teeth to erupt. Without treatment their life expectancy is about 3–5 weeks. In this study we used 6 homozygous *Tcirg1* null and 6 heterozygous/wild type littermates, 18–20 days old, and 2 *Tcirg1* null and 2 adult wild type littermates, 50 days old. These mice were used for gene cell therapy experiments of defective osteoclasts and received Green Fluorescent Protein (GFP) - labelled bone marrow cells at day of birth to rescue osteoclast function [23, 24]. This therapy lead to a partial rescue of the phenotype, resulting in the animals living longer with some bone resorption by GFP-labelled active osteoclasts resulting in tooth eruption, with no effects on dental development (none of the dental cells were GFP- labelled, Bronckers, unpublished results). A strain of adult *anion exchanger-2*-deficient mice of moderate phenotype ($Ae2_{a,b}^{-/-}$ mice) with a mixed 129/Ola and FVB/N background was used as an example of a severely disturbed enamel mineralization [15]. Details of the targeting strategy to generate $Ae2_{a,b}^{-/-}$ mice have been reported elsewhere [25]. All animal handling at the University in Pamplona, Spain and at the Vrije Universiteit Amsterdam, The Netherlands complied with National and International regulations for Animal Care and permission was obtained from the Committee for Animal Care.

Histological procedures

Heads and kidneys were collected and fixed by immersion in 5% paraformaldehyde in 0.1 M phosphate buffer + 2% sucrose overnight. Lower jaws were split into two hemi-mandibles one of which was scanned by microcomputer tomography (microCT, see below). The other hemi-mandibles and maxillae were decalcified in 4.18 % EDTA + 0.8 % formalin at pH 7.2 for two-three weeks at 4°C, rinsed with phosphate buffer, embedded in paraffin along with kidney samples and serially sectioned into 6 μm thick sections.

Immunostaining for v-H-Atpase subunits and enzyme histochemistry of TRAcP

Paraffin sections were stained with haematoxylin-eosin (HE) for a general survey. Selected sections with appropriate stages of enamel development were immunostained by the peroxidase procedure using an ABC Elite kit (Vector Labs, Burlingame, CA, USA) or an Envision kit (Dakopatt, Glostrup, Denmark). The human osteoclast specific TCIRG1 protein has a molecular weight of 110 kDal and contains 720 amino acids. Three different antibodies were used. The first antibody was an affinity purified goat IgG to the human $ATP6V_0$-A_3/TCIRG1 (Santa Cruz, catalogue SC-162300, N13; referred to as ‘’TC-S’’). According to the manufacturer the synthetic peptide used to raise these antibodies was 15–25 amino acids long and maps within the N-terminal-end region, amino acid 75–125 of the human TCIRG1 (NCBI accession number Q13488). The second antibody was an affinity purified rabbit IgG against a 56 amino acids- long recombinant fragment with the sequence

RPADRQEENKAGLLDLPDASVNGWSSDEEKAGGLDDEEEAELVPSEVLMH QAIHTI of the human TCIRG1 (Atlas Antibodies, Sigma, St Louis MO USA, catalogue HPA038742; referred to as ''TC-A"). It locates at amino acid 664–720 of the long isoform of TCIRG1. The third antibody was a rabbit polyclonal antiserum against a 20 amino acids (1–20) long N-terminal peptide of the human ATP6V_1, subunit B_2, (referred to as anti-B2) kindly provided by Dr Shannon Holliday (University of Florida, USA). On western blots from the mouse osteoclast-like cell line (RAW264.7) extracts and isolated mouse v-H-Atpase this antiserum reacts as a single band of the expected size. Working concentrations of the primary antibodies were 1:600–1:800 (anti-B2), 2–4 μg/ml for anti-TC-S and 0.5–1 μg/ml for anti-TC-A. In some studies sections were subjected to antigen retrieval treatment before staining (10 mM citrate pH 6.0, 20 min at 95°C; 1 mM EDTA pH 9.0, 20 min at 95°C; or proteinase K 10 μg/ml in phosphate buffered saline, 20 min a 37°C). Kidney samples contain endogenous biotin that also binds ABC-peroxidase complex [26] especially after antigen retrieval procedures. To suppress false positive staining for endogenous biotin using the ABC-peroxidase method, the kidney sections were first blocked using an avidin biotin blocking kit according to manufacturer's instructions (Vector Labs). To validate specificity of the anti-TCIRG1 antibodies kidney sections from *Tcirg1* null mice were immunostained. As negative controls the primary antibodies were replaced by matched non-immune antibodies from the same species and in the same concentrations. The peroxidase was visualised by DiaminoBenzidine (DAB) staining (brown) after which nuclei were counterstained with methyl green (green-blue) or haematoxylin (blue).To identify osteoclasts, sections were stained red for Tartrate Resistant Acid Phosphatase (TRAcP) using a kit from Sigma.

Microcomputer Tomography (micro CT)

Hemi-mandibles from three 18–20 days old *Tcirg1* null mice and three littermate wild-type or heterozygous mice were scanned at a resolution of 6 μm voxels using a μCT-40 high resolution scanner (Scanco Medical, AG, Bassersdorf, Switzerland) to determine the degree of mineral content in the enamel. Lower incisors of $Ae2_{a,b}$-deficient mice (n=3) and wild type/heterozygous litter mate controls (n=3) were also scanned and measured under identical settings to serve as poorly mineralized enamel due to disruption of the pH regulation in maturation ameloblasts [15]. After scanning a 3-D computer reconstruction of the jaws was made, after which virtual cross-sectioned images were prepared starting at the incisor tip (most developed) into cervical (less developed) direction. In a scout view using steps of 60 μm first the position of the incisors in the jaw tissues was established. Then the slices with the most intensely mineralized enamel were identified (near incisal end, at the level of alveolar bone crest) as area of interest. In this area 1–2 cross-sectioned slices per jaw were selected visually containing the most densely mineralized enamel. Per slice the mineral content of enamel and underlying dentin was measured by point measurements at three sites (Fig. 4). The mean values per mouse were used to calculate an average value (and standard deviation) per group of three mice. The $Ae2_{a,b}^{-/-}$ *mice* were of a different strain and different age than the *Tcirg1* null mice which might affect the quantity of mineral in the dental tissues. We therefore also calculated the ratio between mineral content in enamel and that in underlying dentin to normalize the enamel mineral content for potential (minor) differences in the degree of mineralisation. Statistical significance was tested using Mann-Whitney test ($p \leq 0.05$).

Results

Gross anatomical and histological changes in developing jaws and teeth of Tcirg1 null mutants

The *Tcirg1* null mice were smaller and had a body weight 40% lower than wild type mice (body weights: 11.2 g ± 0.8 g for wild type mice, and 6.6 g ± 1.0 g for *Tcirg1* null mice at postnatal day 18). In *Tcirg1* null mice tooth eruption was severely impaired (Fig. 1a, b). Some bone resorption had occurred which allowed the younger teeth (third molars and some of the second molars) to partially erupt. In wild type littermate mice all molars and incisors had erupted and were functional.

Histologically the *Tcirg1* null mutants were severely osteopetrotic; orofacial bones contained many small marrow cavities instead of few large ones (Fig. 2a1, c, f; Fig 4a, b, e, f). TRAcP staining revealed positive mononuclear and multinuclear cells lining the osteopetrotic bone. Most conspicuously, however, the surface of the osteopetrotic bone was also very strongly labelled for TRAcP (Fig. 2a2).

In *Tcirg1* null mutants all incisors and molars were developing, but root development of the 1st and 2nd molars was severely disrupted and incisors appeared very short in comparison to wild type (one third to one fourth of wild type) (Fig. 2a-f). At the base of the teeth, near the cervical loop, there was only a short distance between the osteopetrotic bone and pulp (Fig. 2c), not seen in wild type controls (Fig 2d, e). In mutants often the dental layer with proliferating cells at the cervical loop of the incisors had folded and the layer became disrupted (Fig. 2f). The fragments formed many islands surrounded by bone tissue but still capable of forming ectopic, small (molar- shaped) teeth (denticles, Fig 2f-j). Ankylosis between dental roots and alveolar bone was locally found in incisors and severely disrupted roots of the first molars (Fig. 2a1).

Though the teeth were often smaller, amelogenesis in *Tcirg1* null mice appeared structurally unaffected, both in the regular teeth and in the forming denticles (Fig. 2g-j). Local defects and disruption of the ameloblast layer was seen at locations where the crowns seemed to be compressed by the osteopetrotic bone. Ameloblasts in all stages looked normal and formed a structured well-organized layer of enamel. The cells deposited substantial amounts of enamel matrix, transformed into maturation ameloblasts, enamel matrix became EDTA soluble and progressively disappeared from the enamel space as seen in wild types.

Immunostaining

To verify the specificity of the antibodies to Tcirg1 we first immunostained kidney tissue sections obtained from wild type and *Tcirg1* null mice. In wild type mice both anti-TC antibodies and the anti-B2 antibody gave intracellular staining in a selection of the epithelial ducts (Fig. 3a, c, and e). The anti-TC-A also stained the nuclei (Fig. 3c). In *Tcirg1*-null mutant kidney anti-TC-S gave no positive staining (Fig. 3b), anti-TC-A stained only the nuclei of the cells (Fig 3d) whereas anti-B2 gave the same positive staining as seen in wild type sections (not shown). Non-immune IgG did not stain any cells in kidney, either in wild type (Fig 3f) or null mutant kidney (not shown).

Anti-TC-A also stained nuclei of the superficial epithelium cells in nasal mucosa (Fig. 3j), nuclei of cells forming ducts of nasal glands and some nuclei in the oral epithelia (not shown), both in wild type and null mutant tissues.

Next we focussed on staining in osteoclasts and ameloblasts. In wild type mice maturation ameloblasts did not react either with anti-TC-S (Fig. 3g, inset) or with anti-TC-A (Fig. 3k). Except for an occasional very faint intracellular reaction using anti-TC-A, antigen retrieval

in citrate buffer could not reveal appreciable staining in these cells. However, the cytoplasm and ruffled border of nearby wild type osteoclasts stained strongly positive (Fig. 3g inset, 3h; Fig. 3k).

Tcirg1 null mutant osteoclasts stained with anti-TC-S were completely negative (Fig. 3i). Whereas in wild type mice the anti-TC-A stained the cytoplasm and the nuclei of osteoclasts (Fig. 3k), in *Tcirg1* null mutant tissues this antibody only stained their nuclei (Fig 3l, m).

Anti-B2 gave a positive staining in maturation ameloblasts (Fig. 3n) and osteoclasts (Fig. 3p, q), in wild types as well as in null mutant mice (Fig. 3o, r, s). In maturation ameloblasts particularly the apical membranes were intensely stained (Fig 3n, r), not seen in osteoclasts in null mutants that stained only intracellular with anti-B2 (Fig. 3s) In contrast to both other antibodies that gave a restricted staining anti-B2 stained more cell- and tissue types in orofacial area including secretory ameloblasts (with a strong staining in their apical parts), stratum intermedium cells, papillary layer (moderate to weak staining, Fig. 3n), epithelial cells lining the nasal cavity (strong), ducts of nasal glands (weak), highly active osteoblasts, young osteocytes, small mononuclear cells around osteoclasts (Fig. 3k), in elongated fibroblasts of mature periodontal ligament (Fig. 3p,q) and some endothelial cells of blood vessel walls (Fig. 3q).

Micro CT analysis

Although teeth in *Tcirg1* null mice were often disfigured and compressed by failure to erupt the microCT analysis showed that mineral content of the most advanced incisor enamel was as high as in wild types (Fig. 4a, b, 5). The same was true for the enamel of molars in *Tcirg1* null mice (Fig. 4e, f). In contrast enamel of $Ae2_{a,b}^{-/-}$ mice used as a positive control for defective enamel mineralisation was much less mineralized (Fig. 4c, d, Fig.5) than wild type controls, even lower than the (unaffected) underlying dentin.

The ratio of mineral content in enamel and that in dentin was the same in *Tcirg1* null mice, the wild type/heterozygous controls to *Tcirg1* null and in wild type controls to $Ae2_{a,b}$-deficient mice (between 1.53–1.55, Fig. 5). In $Ae2_{a,b}$ deficient mice this ratio was significantly lower (0.64) than their wild littermate controls.

Discussion

Maturation ameloblasts and the Tcirg1 subunit

By immunohistochemistry we could not detect osteoclasts-proton pump-specific Tcirg1 ($Atp6v_0a_3$) in mouse ameloblasts, either in secretion or maturation stage. We used two antibodies, each raised against a different part of the human TCIRG1 molecule. The first antibody (anti-TC-S) failed to stain ameloblasts but strongly stained osteoclasts and renal cells in wild type mice but failed to stain these cell types in *Tcirg1*-null mutant mice. The other antibody (TC-A) also did not react with ameloblasts but stained cytoplasm and nuclei of osteoclasts. In null mutant this antibody stained only the nuclei of osteoclasts while also nuclei of several other cell types in null mutant tissues were positive. This data indicates that both the antibodies to human TCIRG1 recognize mouse Tcirg1, that anti-TC-S is specifically detecting Tcirg1 but that anti-TC-A also reacts with an epitope located in nuclei that is not related to mouse Tcirg1.

The v-H-ATPases are involved in a wide variety of physiological processes, including endocytosis, intracellular membrane trafficking, macromolecular processing and degradation, though their primary function is considered to be related to the acidification of intracellular compartments. For their diverse functions, v-H-ATPases utilize specific subunit isoform(s) in specific cells and cell organelles [21, 27, and 28]. The v-H-ATPase complex

exists of two major parts, a V_0 transmembrane part consisting of at least 5 subunits (a, c, c", d and e), and a catalytic cytosolic V_1 component which contains at least 8 subunits (A-H). For osteoclast proton pump activity in mouse the Tcirg1 subunit is essential [9, 20], without which osteoclasts cannot function properly and cannot make pits in bone. The Tcirg1 subunit is however not unique for or exclusively present in osteoclasts or kidney cells, but is most highly expressed in these cells [29] which is consistent with our observations.

Very recently it was reported that *Tcirg1* transcripts are present in secretory stage enamel organ of the rat incisor and that their expression is upregulated in maturation stage [30]. Within the sensitivity of our immunohistochemical technique we could not detect appreciable levels of staining for Tcirg1 in mouse ameloblasts regardless which of both antibodies we used. Both antibodies however did strongly stain osteoclasts and renal epithelial cells. This suggests that even if ameloblasts translate the *Tcirg1* transcripts, the Tcirg1 protein levels are likely very low.

When these antibodies were used to stain developing jaw tissues of rats, hamsters and human foetuses (archival material), both anti-C antibodies were strongly reactive with osteoclasts but not with ameloblasts (unpublished), indicating the present data are not restricted to mice.

We furthermore found no evidence that the functional inactivation of *Tcirg1* in mouse osteoclasts had a clear effect on enamel formation and enamel mineralization.

We conclude from these data that maturation stage ameloblasts do not express appreciable levels of Tcirg1 protein, an essential subunit for functioning of the proton pump in osteoclasts.

Maturation ameloblasts and v-H-Atpase v_1b_2

The v-H-ATP6V_1B_2 localizes to the ruffled border of osteoclasts [22], in line with our observation. We report here that v-H-Atp6v_1b_2 is also located in maturation ameloblasts with strong staining over the ruffled border, similar as reported for v-H-Atpase in rat incisors [14, 16] but we found that this subunit is more widely distributed in murine orofacial tissues than Tcirg1. We speculate that the v-H-Atpase found in rat incisor maturation ameloblasts by Lin et al. [14] and Josephsen et al. [16] is involved in intracellular acidification rather than in plasma membrane proton extrusion. This assumption is consistent with the specifications of the antibodies used by both groups: not against the 116 kD Tcirg1 subunit, but to other subunits shared by more cell types. Lin et al [14] used antibody to ‘’a vacuolar type H-ATPase subunit of 72 kD’ (not further specified but presumably the 70 kD ATP6V_1A, see [21]) and Josephsen et al. [16] used anti-ATP6V_0.A_1, which is highly expressed in brain, neurons, and clathrin-coated vesicles [28], but is lowly expressed in osteoclasts in comparison to ATP6V0A3 [29].

Our data do not support the concept that maturation ameloblasts secrete protons into the enamel space using an osteoclast type of v-H-Atpase but are more in line with our alternate model that maturation ameloblasts secrete bicarbonates neutralizing lowered pH due to proton release from forming minerals [1, 2, 17–19].

Highlights

- Mouse ameloblasts are immunonegative for osteoclast proton pump subunit Tcirg1.
- Mouse osteoclasts are strongly immunopositive for Tcirg1.

- Enamel formation is unaffected in Tcirg1-null (oc/oc) mice.
- It is unlikely that ameloblasts have a proton pump as osteoclasts to acidify matrix.

Acknowledgments

The work was supported by NIH grant RO1 DE013508 (PDB, TB, DL, AB). The authors thank Mr. Peter Brugman for his help with micro computer tomography measurements, and Dr. Shannon Holliday (University of Florida, USA) for providing antibodies to V1B2. Dr. Jing Guo (ACTA, Amsterdam) is acknowledged for help in tissue staining, Dr. Carmen Flores (University of Lund, Sweden) for performing the transplantations in the *Tcirg1* null mice and Dr. Behrouz Zandieh Doulabi for advice on gene and protein structure.

References

1. Smith CE. Cellular and chemical events during enamel maturation. Crit. Rev. Oral. Biol. Med. 1998; 9:128–161. [PubMed: 9603233]
2. Simmer JP, Papagerakis P, Smith CE, Fisher DC, Rountrey AN, Zheng L, Hu JC. Regulation of dental enamel shape and hardness. J. Dent. Res. 2010; 89:1024–1038. [PubMed: 20675598]
3. Nishikawa S, Josephsen K. Cyclic localization of actin and its relationship to junctional complexes in maturation ameloblasts of the rat incisor. Anat. Rec. 1987; 219:21–31. [PubMed: 3688458]
4. Segovia-Silvestre T, Neutzsky-Wul AV, Sorensen MG, Christiansen C, Bollerslev J, Karsdal JA, Henriksen K. Advances in osteoclast biology resulting from the study of osteopetrotic mutants. Hum. Genet. 2009; 124:561–577. [PubMed: 18987890]
5. Helfrich MH. Osteoclast diseases. Microsc. Res. Tech. 2003; 61:514–532. [PubMed: 12879419]
6. Smith CE, Issud M, Margolis HC, Moreno EC. Developmental changes in the pH of enamel fluid and its effects on matrix resident proteinases. Adv. Dent. Res. 1996; 10:159–169. [PubMed: 9206332]
7. Smith CE, Chong DL, Bartlett JD, Margolis HC. Mineral acquisition rates in developing enamel on maxillary and mandibular incisors of rats and mice: implications to extracellular acid loading as apatite crystals mature. J. Bone Miner. Res. 2005; 20:240–249. [PubMed: 15647818]
8. Riihonen R, Supuran CT, Parkkila S, Pastorekova S, Väänänen HK, Laitala-Leinonen T. Membrane-bound carbonic anhydrases in osteoclasts. Bone. 2007; 40:1021–1031. [PubMed: 17291844]
9. Frattini A, Orchard PJ, Sobacchi C, Giliani S, Abinun M, Mattsson JP, Keeling DJ, Andersson AK, Wallbrandt P, Zecca L, Notarangelo LD, Vezzoni P, Villa A. Defects in TCIRG1 subunit of the vacuolar proton pump are responsible for a subset of human autosomal recessive osteopetrosis. Nat. Genet. 2000; 25:343–346. [PubMed: 10888887]
10. Li YP, Chen W, Liang Y, Li E, Stashenko P. Atp6i-deficient mice exhibit severe osteopetrosis due to loss of osteoclast-mediated extracellular acidification. Nat. Genet. 1999; 23:447–451. [PubMed: 10581033]
11. Henriksen K, Gram J, Schaller S, Dahl BH, Dziegiel MH, Bollerslev J, Karsdal MA. Characterization of osteoclasts from patients harboring a G215R mutation in ClC-7 causing autosomal dominant osteopetrosis type II. Am. J. Pathol. 2004; 164:1537–1545. [PubMed: 15111300]
12. Jansen ID, Mardones P, Lecanda F, de Vries TJ, Recalde S, Hoeben KA, Schoenmaker T, Ravesloot JH, van Borren MM MM, van Eijden TM, Bronckers AL, Kellokumpu S, Medina JF, Everts V, Oude Elferink RP. Ae2(a,b)-deficient mice exhibit osteopetrosis of long bones but not of calvaria. FASEB J. 2009; 23:3470–3481. [PubMed: 19564250]
13. Mellis D, Itzstein C, Helfrich M, Crockett JC. The osteoclast: role of key signalling pathways in differentiation and in bone resorption. J. Endocrinol. 2011; 211:131–143. [PubMed: 21903860]
14. Lin HM, Nakamura H, Noda T, Ozawa J. Localization of H+-ATPase and carbonic anhydrase II in ameloblasts at maturation. Calcif. Tissue Int. 1994; 55:38–45. [PubMed: 7922788]

15. Lyaruu DM, Bronckers ALJJ, Mulder L, Mardones P, Medina JF, Kellokumpu S, Oude Elferink RP, Everts V. The anion exchanger Ae2 is required for enamel maturation in mouse teeth. Matrix Biol. 2008; 27:119–127. [PubMed: 18042363]

16. Josephsen K, Takano Y, Frische S, Praetorius J, Nielsen S, Aoba T, Fejerskov O. Ion transporters in secretory and cyclically modulating ameloblasts: a new hypothesis for cellular control of preeruptive enamel maturation. Am. J. Physiol. Cell. Physiol. 2010; 299:C1299–C1307. [PubMed: 20844245]

17. Lacruz RS, Nanci A, Kurtz I, Wright JT, Paine ML. Regulation of pH during amelogenesis. Calcif. Tissue Int. 2010; 86:91–103. [PubMed: 20016979]

18. Bronckers ALJJ, Kalogeraki L, Jorna HJ, Wilke M, Bervoets TJ, Lyaruu DM, Zandieh-Doulabi B, DenBesten P, de Jonge H. The cystic fibrosis transmembrane conductance regulator (CFTR) is expressed in maturation stage ameloblasts, odontoblasts and bone cells. Bone. 2010; 46:1188–1196. [PubMed: 20004757]

19. Bronckers ALJJ, Guo J, Zandieh-Doulabi B, Bervoets TJ, Lyaruu DM, Li X, Wangemann P, DenBesten P. Developmental expression of SLC24A4 (pendrin) during amelogenesis in developing teeth. Eur. J. Oral Sci. 2011; 119(supplement 1):185–195. [PubMed: 22243245]

20. Scimeca JC, Franch A, Trojani C, Parrinello H, Grosgeorge J, Robert C, Jaillon O, Poirier C, Gaudray P, Carlei GF. The gene encoding the mouse homologue of the human osteoclast specific 116-kDa V-H-ATPase subunit bears a deletion in osteosclerotic (oc/oc) mutants. Bone. 2000; 26:207–213. [PubMed: 10709991]

21. Xu J, Cheng T, Feng HT, Pavlos NJ, Zheng MH. Structure and function of v-ATPases in osteoclasts: potential therapeutic targets for the treatment of osteolysis. Histol. Histopath. 2007; 22:443–454.

22. Mattsson JP, Skyman C, Palokangas H, Väänänen KH, Keeling DJ. Characterization and cellular distribution of the osteoclast ruffled membrane vacuolar- H-ATPase B-subunit using isoform-specific antibodies. J. Bone Miner. Res. 1997; 12:753–760. [PubMed: 9144341]

23. Johansson MK, de Vries TJ, Schoenmaker T, Ehinger M, Brun AC, Fasth A, Karlsson S, Everts V, Richter J. Hematopoietic stem cell-targeted neonatal gene therapy reverses lethally progressive osteopetrosis in *oc/oc* mice. Blood. 2007; 109:5178–5185. [PubMed: 17332244]

24. Flores C, de Vries TJ, Moscatelli I, Askmyr M, Schoenmaker T, Langenbach GE, Ehinger M, Everts V, Richter J. Nonablative neonatal bone marrow transplantation rapidly reverses severe murine osteopetrosis despite low-level engraftment and lack of selective expansion of the osteoclastic lineage. J. Bone Miner. Res. 2010; 25:2069–2077. [PubMed: 20568230]

25. Medina JF, Recalde S, Prieto J, Lecanda J, Saez E, Funk CD, Vecino P, van Roon MA, Ottenhof R, Bosma PJ, Bakker CT, Oude-Elferink RP. Anion exchanger 2 is essential for spermiogenesis in mice. Proc. Natl. Acad. Sci. USA. 2003; 100:15847–15852. [PubMed: 14673081]

26. Vosse A, Seelentag W, Bachmann A, Bosman FT, Yan P. Background staining of visualization systems in immunohistochemistry: comparison of the Avidin-Biotin Complex system and the EnVision+ system. Appli. Immunohistochem. Mol. Morphol. 2007; 15:103–106.

27. Wu H, Xu G, Li Y. Atp6vd2 is an essential component of the osteoclast-specific proton pump that mediates extracellular acidification in bone resorption. J. Bone Miner. Res. 2009; 24:871–885. [PubMed: 19113919]

28. Rahman S, Ishizuka-Katsura Y, Arai S, Saijo S, Yamato I, Toyama M, Ohsawa N, Inoue M, Honda K, Terada T, Shirouzu M, Yokoyama S, Iwata S, Murata T. Expression, purification and characterization of isoforms of peripheral stalk subunits of human V-ATPase. protein Expr. Purif. 2011; 78:181–188. [PubMed: 21356312]

29. Nyman JKE, Väänänen KH. A rationale for osteoclast selectivity of inhibiting the lysosomal V-ATPase a3 isoform. Calcif. Tissue Int. 2010; 87:273–283. [PubMed: 20596699]

30. Lacruz RS, Smith CE, Bringas P, Chen YB, Smith SM, Snead ML, Kurtz I, Hacia JG, Hubbard MJ, Paine ML. Identification of novel candidate genes involved in mineralization of dental enamel by genome-wide transcript profiling. J Cell Physiol. 2011 Aug 1. [Epub ahead of print].

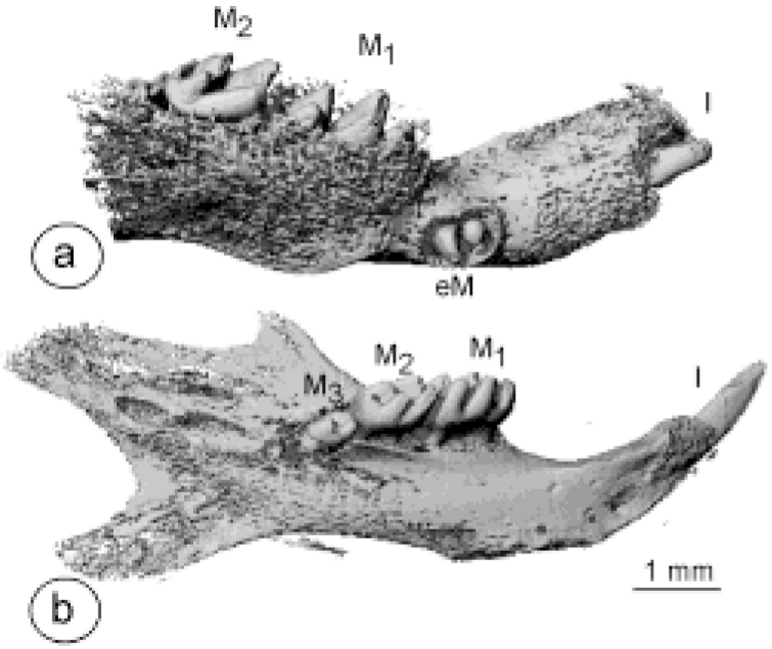

Fig. 1. a, b. A microCT image of the mandible of an 18 days old *Tcirg1* null mouse (a) and a control wild type littermate (b)

In the mutant mouse the incisor (I) is just emerging beyond the bony crest. Also the tips of first (M_1) and second (M_2) molars are becoming apparent above the bone surface. An ectopical molar (eM) denticle is forming near the cervical loop area of the shortened incisor.

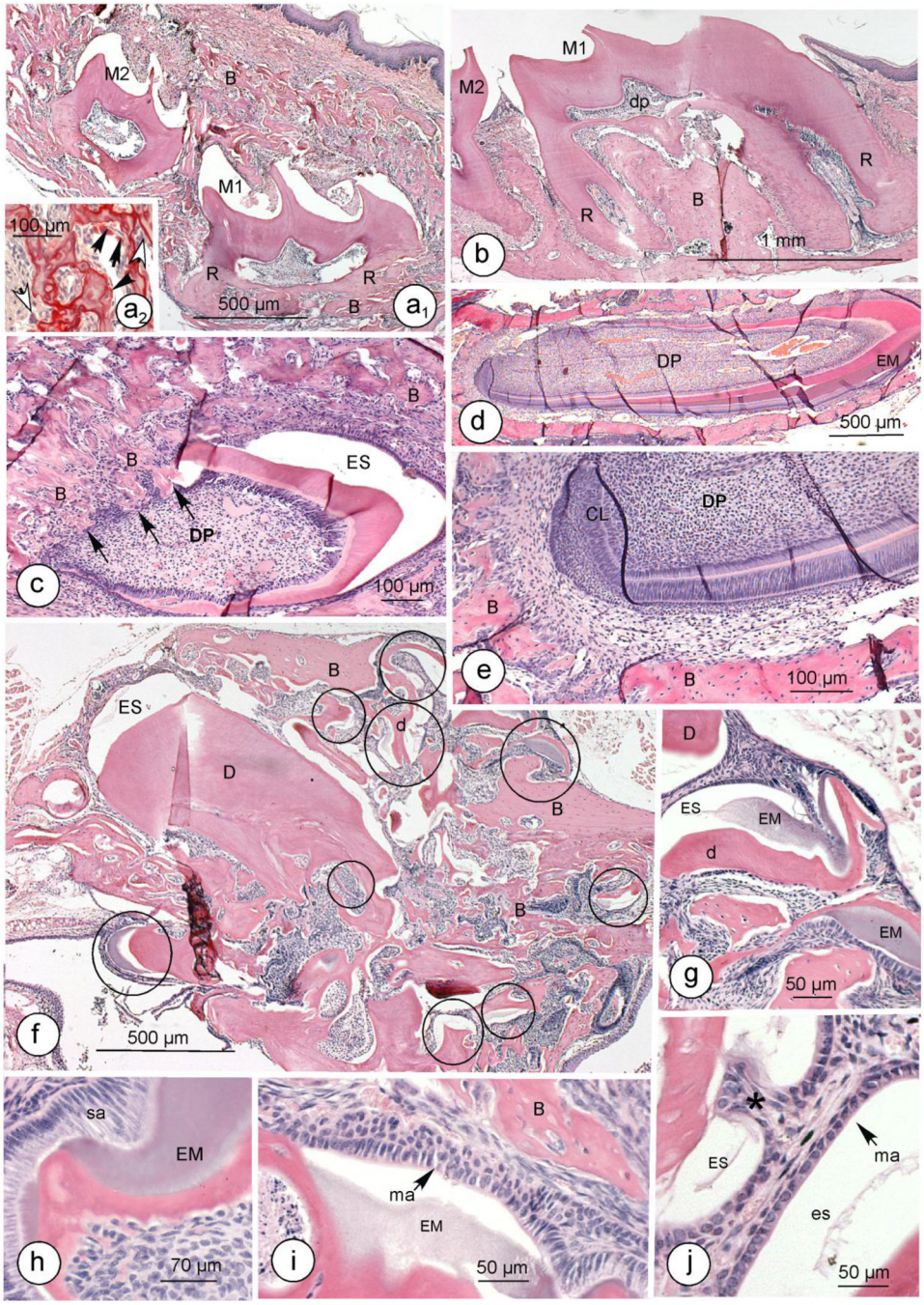

Fig. 2. Histological changes in tooth development in osteopetrotic mice

Fig.2a1. Unerupted first (M1) and second (M2) molars surrounded by osteopetrotic bone (B) of a *Tcirg1*- null mouse (x 50). Roots (R) of M1 have fused with bone. Fig 2a2: TRAcP staining of osteopetrotic bone. Intense staining is located at the bone margins. Black arrow heads point at TRAcP positive mononuclear and multinuclear osteoclasts. White arrow heads indicate multinuclear cells that are TRAcP negative (x 400). Fig. 2b. Wild type littermate to mouse in Fig 2a1. Molars (M1, M2) with normal roots (R) have erupted into oral cavity (x 50). Fig. 2c. A developing molar crown of a *Tcirg1*- null mouse at an unusually close distance from surrounding osteopetrotic bone. At the base of the molar the bone almost invades (arrows) the dental pulp (DP) (x 100). Fig. 2d (x 25), 2e (x 100): Wild

type incisor with normal relatively wide space between cervical loop (CL) and bone (B). The cervical loop is shown at higher magnification in Fig. 2e. Fig. 2f. Impacted incisor of *Tcirg1*- null mouse with enamel space (ES) and dentin (D) (x 50). Its cervical loop has disrupted and fragments encapsulated by osteopetrotic bone have formed multiple scattered ectopic small denticles (circles) in all stages of enamel development. Denticles are shown in detail in Figs 2g-j (Fig 2g:×100: Figs 2h, j.×400, Fig 4i.×250). Small enamel defects (*, Fig 2j) by local disruption of ameloblasts are occasionally seen. Abbreviations:B bone; CL cervical loop; D dentin; DP dental pulp; EM enamel matrix, ES enamel space; M1 first molar; ma maturation ameloblasts, R root; sa secretory ameloblasts. Hematoxylen staining. All magnifications indicated as original magnifications.

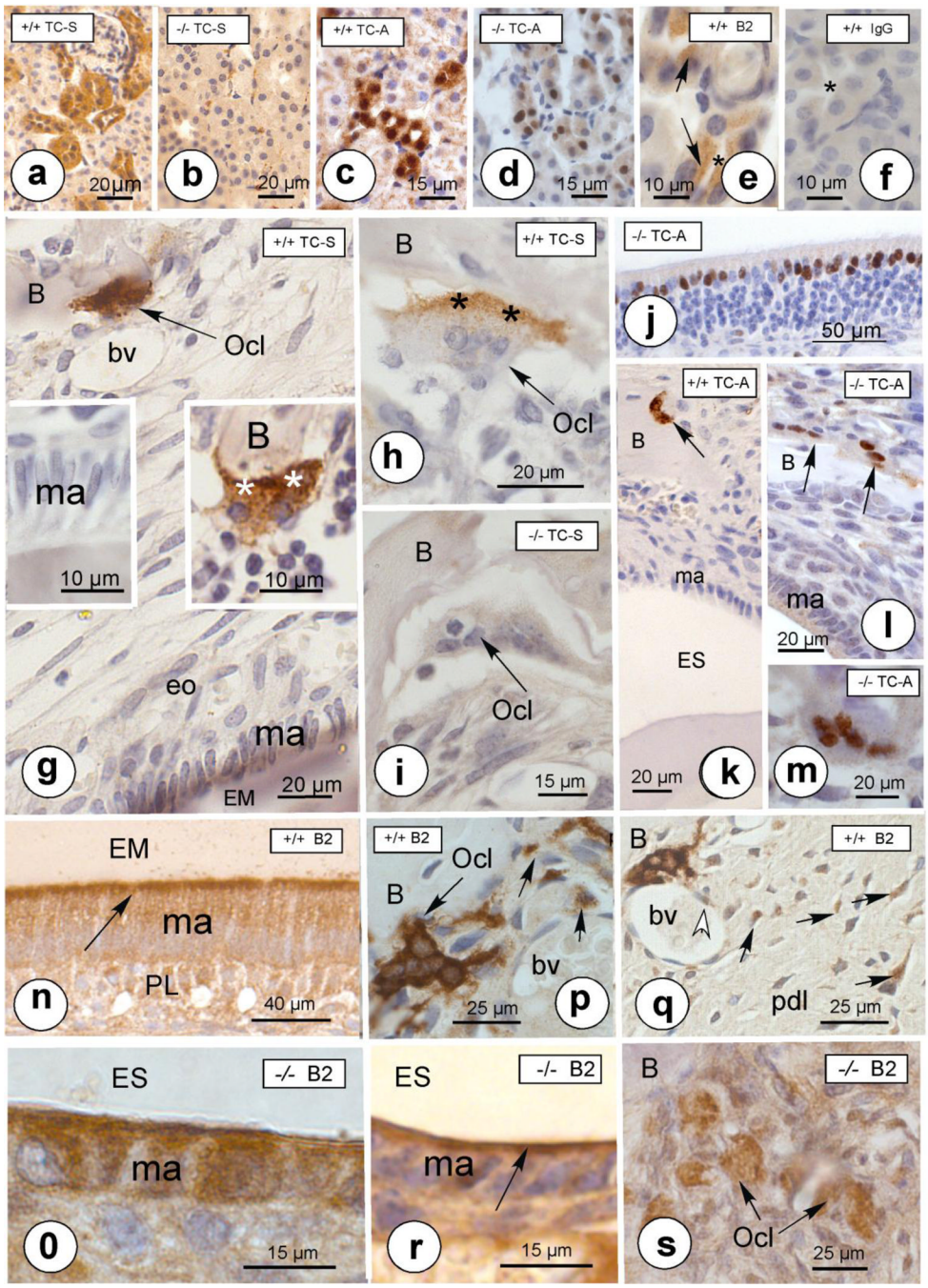

Fig. 3. Validation of anti-TCIRG1 and anti-ATP6V1B2 on *Tcirg1* null kidney sections (Fig. 3a-f) and staining patterns of osteoclasts and ameloblasts with different antibodies in jaw tissues (Fig 3g-s)

Fig. 3a: Wild type (+/+) kidney tubular epithelium stained with anti-TCIRG1-S (Fig. 3a, referred to as TC-S;×400), anti-TCIRG1-A (Fig 3c, 'TC-A',×400) or anti-v-H-ATP6V_1B_2 (Fig. 3e, 'B2',×1000). In fig. 3e: asterisk indicates lumen of tubule; arrows point at positive staining. *Tcirg1* null mutant (−/−) kidney stained with anti-TC-S (Fig 3b,×400) or anti-TC-A (Fig. 3d,×400). As control wild type kidney as stained with non-immune rabbit IgG (Fig. 3f,×1000). Figs 3g, h. Osteoclasts (Ocl) but not (incisor) maturation ameloblasts (ma) in developing wild type jaws anti-TC-C. Asterisks: ruffled border. The maturation ameloblasts

are partly covered by a detached part of dentin matrix. An osteoclast in null mutant tissue is immunonegative with anti-TC-S (Fig. 3i,×1000). Fig. 3k (x 400): Positive staining of cytoplasm and nuclei of an osteoclast (arrow) with anti-TC-A, but not in maturation ameloblasts (ma) of a wild type mouse. Fig. 3j (superficial layer of nasal epithelium,×200), 3l (x 400) and 3m (x 1000) show positive nuclear staining in osteoclasts (arrows) and nasal epithelium in null mutant jaw reacted with anti-TC-A. Figs 3n-s: Cells stained with anti-B2. In wild type jaw anti-B2 stains maturation ameloblasts (ma) in particular the apical membrane (arrow) (Fig 3n,×400), multinucleated osteoclasts and small mononucleated fibroblast-like cells in periodontal space (arrows, Figs 3p, q,×400) and endothelial cells (Fig. 3q white arrow head). In null mutant mice anti-B2 stained cytoplasm (Fig 3o,×1000), and apical membranes (arrow, Fig 3r,×1000) of maturation ameloblasts (ma) in denticles and multinuclear osteoclasts in osteopetrotic bones (Fig 3s;×400). Abbreviations: B bone, BV blood vessel, EM enamel matrix, EO enamel organ; EM enamel matrix; ES enamel space; ma maturation ameloblasts; PL papillary layer; Ocl osteoclast

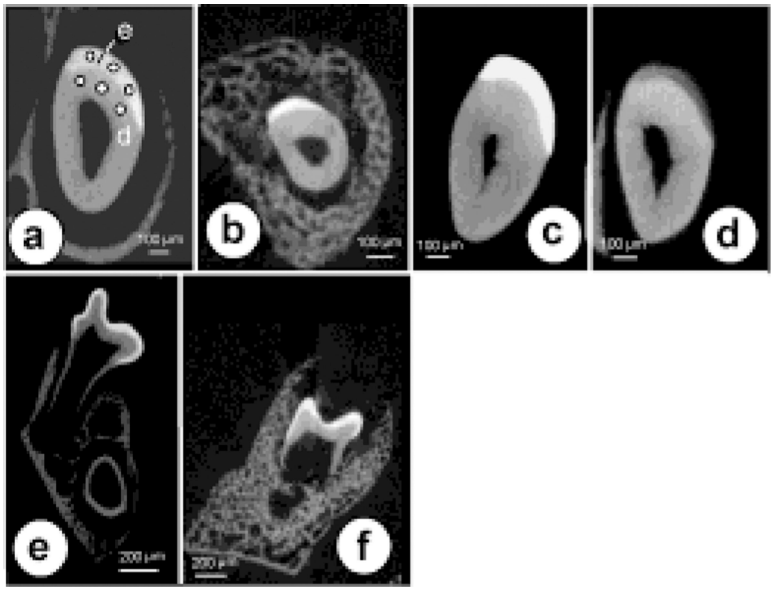

Fig. 4. MicroCt images of cross-sections through mandibular incisors (a-d) and molars (e, f)

Fig. 4a is from a digital reconstruction of a wild type and fig. 4b from a *Tcirg1*- null mouse, both 18 days old. The small circles in enamel (e) and dentin (d) in fig. 4a indicate the locations where measurements have been taken. Enamel in both control and mutant mouse is well mineralized. Figs 4c and 4d are cross sections through incisor of control and an $Ae2_{a,\,b}^{-/-}$ mouse, 9 weeks old. Enamel in the *Ae2a,b* null mutant mouse is poorly mineralized. Figs 4e and 4f are cross sections through the first molar of a control (Fig. 4e) and *Tcirg1*- null mutant (Fig. 4f). A thick layer of bone is still present around the roots in the mutant jaw (Fig. 4f). The enamel in the *Tcirg1*- null mutant is well mineralized.

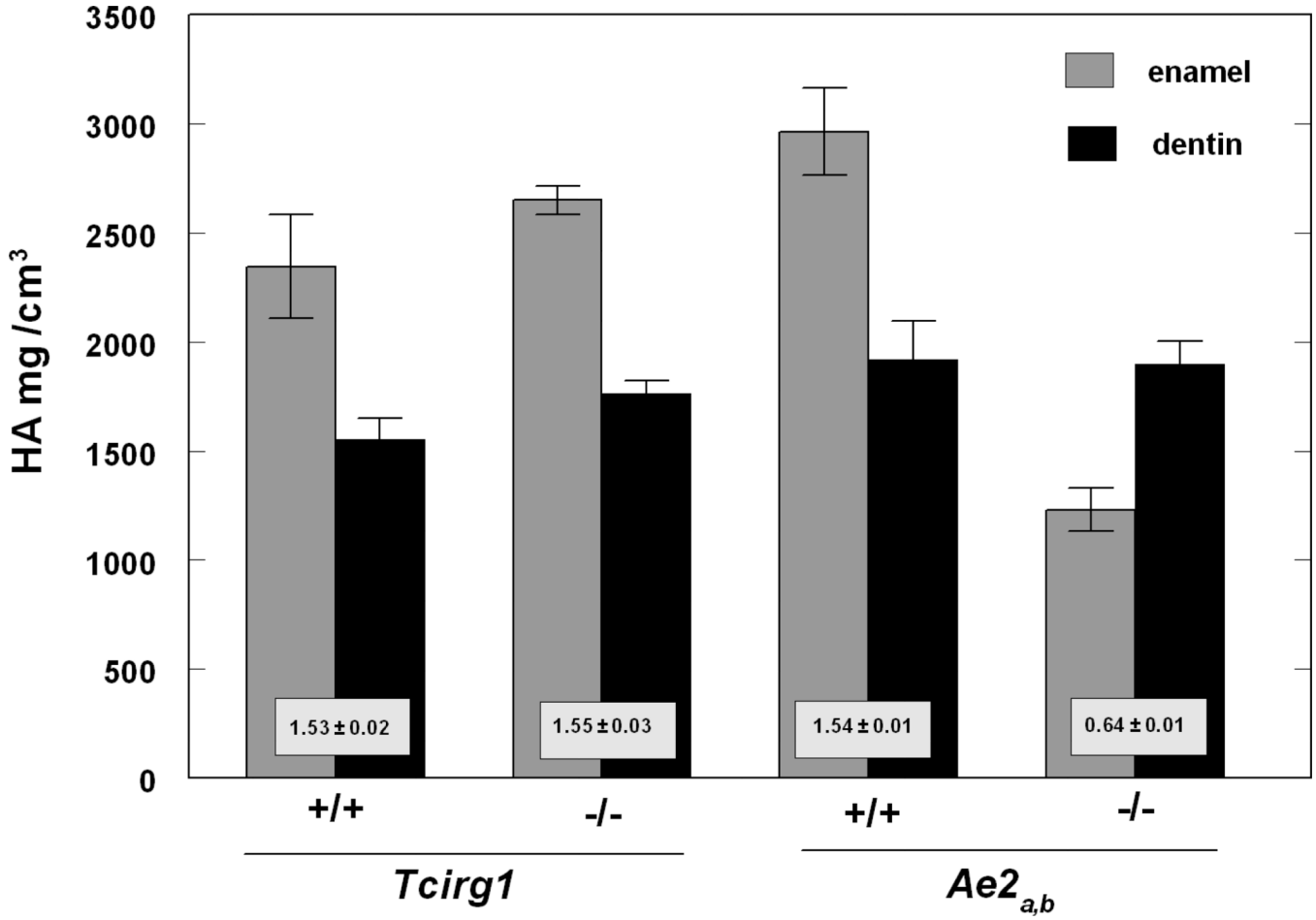

Fig. 5. Comparison of mineral content of incisor enamel between *Tcirg1*- null mice, $Ae2_{a,b}$ deficient mice and their wild type /heterozygous littermate controls assessed by microCT

The *Tcirg1*- null mice were 18–20 days old, the $Ae2_{a,b}$ deficient mice 9 weeks old. The Y-axis represents mineral content expressed as mg hydroxyapatite (HA) per cubic cm. The values in the boxes represent enamel/dentin ratio's (Means and SD, n=3). Only the mineral content in enamel of the $Ae2_{a,b}$ deficient mice is significantly lower than that in controls ($p<0.05$).